Report no. 04/18

The Importance of Adjoint Consistency in the Approximation of Linear Functionals Using the Discontinuous Galerkin Finite Element Method

Kathryn Harriman, David Gavaghan and Endre Süli

We describe how a discontinuous Galerkin finite element method with interior penalty can be used to compute the solution to an elliptic partial differential equation and a linear functional of this solution can be evaluated. We show that, in order to have an adjoint consistent method and thus obtain optimal rates of convergence of the functional, a symmetric interior penalty Galerkin method must be used and, when the functional depends on the derivative of the solution of the PDE, an equivalent formulation of the functional must be used.

Key words and phrases: Finite element methods, discontinuous Galerkin methods, linear functionals, adjoint consistent, dual problem

Oxford University Computing Laboratory
Numerical Analysis Group
Wolfson Building
Parks Road
Oxford, England OX1 3QD

July, 2004

1 Introduction

In many areas of application the aim of a computation is not to approximate the solution to the governing partial differential equation system but rather to compute accurately a linear functional or series of linear functionals of their solution. Such linear functionals might take the form of a flux through an outflow boundary, the local mean value of a field or a point evaluation. Specific areas of application include:

- Fluid dynamics — estimation of the lift and drag coefficients of a body immersed in a viscous incompressible fluid whose flow is governed by the Navier Stokes equations [7];
- Elasticity theory — estimation of the stress intensity factor or the moments of a shell or a plate [1, 2, 3];
- Radiative transfer — estimation of a scalar flux or a limited number of flow intensities in arbitrary directions [6];
- Electrochemistry — estimation of the current flowing at a working electrode [8, 9].

Here, we shall use the discontinuous Galerkin finite element method for solving the governing partial differential equation and we discuss how to 'post-process' the solution in order to estimate the linear functional accurately.

Discontinuous Galerkin finite element methods (DGFEMs) were first introduced in the early 1970's. The method was proposed by Reed & Hill [15] in 1973 for the numerical solution of the neutron transport equation and also by Nitsche [12] in 1971 as nonstandard schemes for the approximation of second-order elliptic equations. Since then much work has been undertaken to develop these methods for a range of problems; for more details see the review article by Cockburn *et al.* [4].

DGFEM has several key advantages over the standard finite element method. The first is that, since the solution is allowed to be discontinuous across inter-element boundaries, variation in polynomial degree between elements is easily implemented. This makes the method an ideal candidate as the basis for an adaptive *hp*-refinement algorithm. A second important advantage of the discontinuous method is that there is no need to use streamline diffusion when dealing with convection-dominated diffusion problems. This means that reaction-diffusion and reaction-convection-diffusion problems may be treated in a uniform manner.

The aim of this work is to compare several different ways of computing the linear functional. We shall use an interior penalty discontinuous Galerkin method to solve the governing partial differential equation. The interior penalty method will lead to either a symmetric or nonsymmetric bilinear form, however we shall demonstrate that the symmetric version performs better since it leads to an adjoint-consistent method. We also demonstrate that if the functional depends on the derivative of the solution, rather than the solution itself, it is helpful to rewrite the functional in a formulation which is equivalent at the continuous level but leads to numerical approximations which converge at a faster rate. Again this is because we are ensuring adjoint consistency.

The paper is structured as follows. In Section 2 we introduce the model problem and formulate its discontinuous Galerkin finite element approximation. In Section 3 an *a priori* bound on the error in the computed functional is stated and the dual problem is described. In Section 4 we give details of the dual problem for specific functionals paying particular attention to the case of a flux across a portion of the boundary. In Section 5 we present some numerical examples and finally, in Section 6 we summarise the work presented in this paper and draw some conclusions.

2 Model Problem

Let Ω be a bounded open domain in $\mathbb{R}^d$ and let Γ be the union of its $(d-1)$-dimensional open faces. We consider the (elliptic) reaction-diffusion equation

$$\mathcal{L}u \equiv -\nabla^2 u + Ku = f \,, \tag{2.1}$$

where $f \in L_2(\Omega)$ and K is a nonnegative constant. We denote by $\mathbf{n}(x) = \{n_i(x)\}_{i=1}^d$ the outward unit normal vector to Γ at $x \in \Gamma$. Then (2.1) is supplemented with boundary conditions

$$u = g_{\mathrm{D}} \qquad \text{on } \Gamma_{\mathrm{D}} \,, \tag{2.2a}$$

$$\nabla u \cdot \mathbf{n} = g_{\mathrm{N}} \qquad \text{on } \Gamma_{\mathrm{N}} \,, \tag{2.2b}$$

where we assume that Γ_{D} and Γ_{N} are disjoint subsets with union Γ. We also assume that Γ_{D} is nonempty.

2.1 Meshes, Finite Element Spaces and Notation

We consider shape-regular meshes $\mathcal{T}_h = \{\alpha\}$ that partition the domain Ω into open element domains α. Hanging nodes are allowed, although we shall assume that there is at most one hanging node per element-face which we assume to be the barycenter of the face. We denote by h the piecewise constant mesh function with $h(x) \equiv h_\alpha = \mathrm{diam}(\alpha)$ for $x \in \alpha$. We assume that each element $\alpha \in \mathcal{T}_h$ is a smooth bijective image of a fixed reference element $\hat{\alpha} = (-1,1)^d$, that is, $\alpha = F_\alpha(\hat{\alpha})$ for all $\alpha \in \mathcal{T}_h$. On $\hat{\alpha}$ we define $\mathcal{Q}_p$ to be the space of polynomials of degree $p \geq 1$ in each of the d coordinate directions:

$$\mathcal{Q}_p = \mathrm{span}\left\{\hat{x}^\beta : 0 \leq \beta_i \leq p, \;\; 1 \leq i \leq d\right\} \,.$$

To each $\alpha \in \mathcal{T}_h$ we assign an integer $p_\alpha \geq 1$; collecting the p_α and F_α in the vectors $\mathbf{p} = \{p_\alpha : \alpha \in \mathcal{T}_h\}$ and $\mathbf{F} = \{F_\alpha : \alpha \in \mathcal{T}_h\}$, respectively, we introduce the finite element space

$$S^{\mathbf{p}}(\Omega, \mathcal{T}_h, \mathbf{F}) = \{u \in L_2(\Omega) \,:\, u|_\alpha \circ F_\alpha \in \mathcal{Q}_{p_\alpha};\; \alpha \in \mathcal{T}_h\} \,.$$

Associated with $\mathcal{T}_h$, we introduce the broken Sobolev space of composite order $\mathbf{s}$ defined by

$$H^{\mathbf{s}}(\Omega, \mathcal{T}_h) = \{u \in L_2(\Omega) : \; u|_\alpha \in H^{s_\alpha}(\alpha) \quad \forall \alpha \in \mathcal{T}_h\} \,,$$

equipped with the broken Sobolev norm and corresponding semi-norm, respectively,

$$\|u\|_{\mathbf{s},\mathcal{T}_h} \;=\; \Big(\sum_{\alpha\in\mathcal{T}_h} \|u\|^2_{H^{s_\alpha}(\alpha)}\Big)^{1/2}, \qquad |u|_{\mathbf{s},\mathcal{T}_h} \;=\; \Big(\sum_{\alpha\in\mathcal{T}_h} |u|^2_{H^{s_\alpha}(\alpha)}\Big)^{1/2}. \tag{2.3}$$

When $s_\alpha = s$ for all $\alpha \in \mathcal{T}_h$, we write $H^s(\Omega,\mathcal{T}_h)$, $\|u\|_{s,\mathcal{T}_h}$ and $|u|_{s,\mathcal{T}_h}$.

An *interior face* of $\mathcal{T}_h$ is defined as the (non-empty) $(d-1)$–dimensional interior of $\partial\alpha_i \cap \partial\alpha_j$, where α_i and α_j are two adjacent elements of $\mathcal{T}_h$, not necessarily matching. A *boundary face* of $\mathcal{T}_h$ is defined as the (non-empty) $(d-1)$–dimensional interior of $\partial\alpha\cap\Gamma$, where α is a boundary element of $\mathcal{T}_h$. We denote by $\Gamma_{\rm int}$ the union of all interior faces of $\mathcal{T}_h$. Given a face $e \subset \Gamma_{\rm int}$, shared by the two elements α_i and α_j, where the indices i and j satisfy $i > j$, we write $\mathbf{n}_e$ to denote the (numbering–dependent) unit normal vector which points from α_i to α_j; on boundary faces, we put $\mathbf{n}_e = \mathbf{n}$. Further, for $v \in H^1(\Omega,\mathcal{T}_h)$ we define the jump of v across e and the mean value of v on e, respectively, by

$$[v] = v|_{\partial\alpha_i\cap e} - v|_{\partial\alpha_j\cap e} \quad \text{and} \quad \langle v\rangle = \frac{1}{2}\left(v|_{\partial\alpha_i\cap e} + v|_{\partial\alpha_j\cap e}\right). \tag{2.4}$$

On a boundary face $e \subset \partial\alpha$, we set $[v] = v|_{\partial\alpha\cap e}$ and $\langle v\rangle = v|_{\partial\alpha\cap e}$.

2.2 The *hp*-Discontinuous Galerkin Method

The *hp*-DGFEM approximation of (2.1), (2.2) is defined as follows: find $u_{\rm DG}$ in $S^{\mathbf{p}}(\Omega,\mathcal{T}_h,\mathbf{F})$ such that

$$B_{\rm DG}(u_{\rm DG},v) = \ell_{\rm DG}(v) \tag{2.5}$$

for all $v \in S^{\mathbf{p}}(\Omega,\mathcal{T}_h,\mathbf{F})$. The bilinear form $B_{\rm DG}(\cdot,\cdot)$ is defined by

$$\begin{aligned} B_{\rm DG}(w,v) \;=\; & \sum_{\alpha\in\mathcal{T}_h}\int_\alpha (\nabla w\cdot\nabla v + Kwv)\,{\rm d}\Omega \\ & - \int_{\Gamma_{\rm int}\cup\Gamma_{\rm D}} \left(\langle\nabla w\cdot\mathbf{n}_e\rangle\,[v] - \theta\langle\nabla v\cdot\mathbf{n}_e\rangle\,[w]\right){\rm d}s + \int_{\Gamma_{\rm int}\cup\Gamma_{\rm D}} \sigma\,[w]\,[v]\,{\rm d}s\,, \end{aligned} \tag{2.6}$$

and the linear functional $\ell_{\rm DG}(\cdot)$ is given by

$$\ell_{\rm DG}(v) \;=\; \sum_{\alpha\in\mathcal{T}_h}\int_\alpha fv\;{\rm d}\Omega + \int_{\Gamma_{\rm N}} g_{\rm N}v\;{\rm d}s + \int_{\Gamma_{\rm D}} (\theta\nabla v\cdot\mathbf{n} + \sigma v)\,g_{\rm D}\;{\rm d}s\,. \tag{2.7}$$

Here, σ is called the *discontinuity-penalisation* parameter, and is defined by

$$\sigma|_e \;=\; C_\sigma\frac{\langle p^2\rangle}{h_e} \text{ for } e\subset\Gamma_{\rm int}\cup\Gamma_{\rm D}\,, \tag{2.8}$$

where h_e is the length of edge e and C_σ is a positive constant, cf. [11].

Selecting the parameter $\theta = 1$ gives rise to the so–called *Nonsymmetric Interior Penalty Galerkin (NIPG) method*, while setting $\theta = -1$ yields the *Symmetric Interior*

Penalty Galerkin (SIPG) scheme. The SIPG scheme seems the natural choice since a symmetric operator is represented by a symmetric bilinear form which is not the case with the NIPG method. However, the symmetric scheme has the slight drawback that it requires $C_\sigma > C'_\sigma > 0$ where C'_σ is a sufficiently large positive constant, in order to ensure coercivity of the bilinear form with respect to the norm $|||\cdot|||_{\rm DG}$ defined by

$$\begin{aligned} |||w|||^2_{\rm DG} &= \sum_{\alpha\in\mathcal{T}_h}\int_\alpha \left(|\nabla w|^2 + K|w|^2\right)\,{\rm d}\Omega + \int_{\Gamma_{\rm int}\cup\Gamma_{\rm D}} \sigma\,[w]^2\,{\rm d}s \\ &\quad + \int_{\Gamma_{\rm int}\cup\Gamma_{\rm D}} \sigma^{-1}\langle\nabla w\cdot\mathbf{n}_\alpha\rangle^2\,{\rm d}s\ . \end{aligned} \tag{2.9}$$

The NIPG method can be shown to be coercive for any nonnegative value of C_σ. For a proof of these results, see Ref. [14].

3 An *A Priori* Error Bound

Given that we have the solution u to the problem given by (2.1) and (2.2) we wish to evaluate the linear function $J(u)$. We assume that $J(u)$ is a linear functional of either the solution u itself or the first derivatives of the solution $\partial u/\partial x_i$, $i = 1,\ldots,d$. The dual problem then requires us to find $w \in H^2(\Omega,\mathcal{T}_h)$ such that

$$B_{\rm DG}(\phi, w) = J(\phi) \quad \forall\phi \in H^2(\Omega,\mathcal{T}_h)\ . \tag{3.1}$$

Based on this dual problem, an *a priori* error bound can be derived on the error in the computed functional. The method is the same as for reaction-convection-diffusion equations, and was described in [10]. We assume that the primal solution satisfies $u|_\alpha \in H^{s_\alpha}(\alpha)$ for $\alpha\in\mathcal{T}_h$ and that the dual solution corresponding to the SIPG method satisfies $w^{\rm SIPG}|_\alpha \in H^{t_\alpha}(\alpha)$ for $\alpha\in\mathcal{T}_h$ where $s_\alpha, t_\alpha \geq 2$. The *a priori* error bound is then given by

$$\begin{aligned} |J(u) - J(u_{\rm DG})|^2 &\leq C\sum_\alpha \left(\frac{h_\alpha^{2\mu_\alpha-2}}{p_\alpha^{2s_\alpha-3}} + K\frac{h_\alpha^{2\mu_\alpha}}{p_\alpha^{2s_\alpha}}\right)\|u\|^2_{H^{s_\alpha}}(\alpha) \\ &\times\left(\sum_\alpha\left(\frac{h_\alpha^{2\bar\mu_\alpha-2}}{p_\alpha^{2t_\alpha-3}} + K\frac{h_\alpha^{2\bar\mu_\alpha}}{p_\alpha^{2t_\alpha}}\right)\|w^{\rm SIPG}\|^2_{H^{t_\alpha}}(\alpha) + (1+\theta)\|w^{\rm SIPG}\|^2_{H^2(\mathcal{T}_h)}\right), \end{aligned} \tag{3.2}$$

where $\mu_\alpha = \min(s_\alpha, p_\alpha+1)$ and $\bar\mu_\alpha = \min(t_\alpha, p_\alpha+1)$.

In the special case of a uniform mesh ($h_\alpha = h$, $p_\alpha = p$) and uniform regularity of the solution ($s_\alpha = s$ and $t_\alpha = t$ so that $\mu_\alpha = \mu$ and $\bar\mu_\alpha = \bar\mu$) we have

$$\begin{aligned} |J(u) - J(u_{\rm DG})| &\leq C\frac{h^{\mu+\bar\mu-2}}{p^{s+t-2}}p\|u\|_{H^s(\Omega)}\|w\|_{H^t(\Omega)} \\ &\quad + (1+\theta)\frac{h^{\mu-1}}{p^{s-3/2}}\|u\|_{H^s(\Omega)}\|w^{\rm SIPG}\|_{H^2(\Omega)}\ . \end{aligned} \tag{3.3}$$

This shows that for SIPG we have

$$|J(u) - J(u_{\mathrm{DG}})| \;=\; \mathcal{O}(h^{\mu+\bar{\mu}-2}) \,, \tag{3.4}$$

whilst for NIPG we have only

$$|J(u) - J(u_{\mathrm{DG}})| \;=\; \mathcal{O}(h^{\mu-1}) \,. \tag{3.5}$$

4 Specific Functionals

We shall consider three specific types of functional: the weighted mean value of a field; a point value; and a flux through part of the boundary of the domain. We then define

$$J_1(u) \;=\; \int_\Omega \psi_1(x) u(x) \,\mathrm{d}\Omega \,, \tag{4.1}$$

$$J_2(u) \;=\; u(x_0) \,, \tag{4.2}$$

$$J_3(u) \;=\; \int_{\Gamma_0} \psi_3(x) \nabla u \cdot \mathbf{n} \,\mathrm{d}s \,, \tag{4.3}$$

where $\psi_1 \in L_2(\Omega)$, $x_0 \in \Omega$, $\psi_3 \in H_{00}^{1/2}(\Gamma_0)$ and we assume that $\Gamma_0 \subset \Gamma_{\mathrm{D}}$ since $\nabla u \cdot \mathbf{n}$ is known exactly on Γ_{N}.

The dual problems are then given by

$$B(\phi, w) \;=\; J_i(\phi), \quad i = 1, 2, 3. \tag{4.4}$$

Performing integration by parts we see that the dual problem corresponding to the functional $J_1(\cdot)$ is: find w such that

$$\mathcal{L}^\star w \;\equiv\; -\nabla^2 w + Kw \;=\; \psi_1 \quad \text{in } \alpha \,, \tag{4.5}$$

with inter-element conditions

$$(1+\theta)\langle \nabla w \cdot \mathbf{n}_\alpha \rangle + \sigma\,[w] \;=\; 0 \quad \text{on } \partial\alpha \setminus \Gamma \,, \tag{4.6a}$$

$$[w] \;=\; 0 \quad \text{on } \partial\alpha \setminus \Gamma \,, \tag{4.6b}$$

and boundary conditions

$$w \;=\; 0 \quad \text{on } \partial\alpha \cap \Gamma_{\mathrm{D}} \,, \tag{4.7a}$$

$$\nabla w \cdot \mathbf{n}_\alpha \;=\; 0 \quad \text{on } \partial\alpha \cap \Gamma_{\mathrm{N}} \,, \tag{4.7b}$$

$$(1+\theta)\nabla w \cdot \mathbf{n}_\alpha \;=\; 0 \quad \text{on } \partial\alpha \cap \Gamma_{\mathrm{D}} \,, \tag{4.7c}$$

for all $\alpha \in \mathcal{T}_h$.

We observe that when $\theta = -1$ the inter-element conditions (4.6) simply state that the dual solution should be continuous across inter-element boundaries and thus there is no dependence on the mesh.

The dual problem corresponding to the functional $J_2(\cdot)$ is: find w such that

$$\mathcal{L}^\star w \equiv -\nabla^2 w + Kw = \begin{cases} \delta(x-x_0) & \text{in } \alpha \text{ if } x_0 \in \alpha \\ 0 & \text{in } \alpha \text{ if } x_0 \notin \alpha \,, \end{cases} \tag{4.8}$$

with inter-element conditions and boundary conditions given by (4.6) and (4.7).

Finally, we consider the dual problem for the functional $J_3(\cdot)$. The dual solution must satisfy

$$-\nabla^2 w = 0 \quad \text{in } \alpha \,, \tag{4.9}$$

with inter-element conditions given by (4.6) and boundary conditions given by

$$w = \begin{cases} -\psi_3(x,y) & \text{on } \partial\alpha \cap (\Gamma_D \cap \Gamma_0) \,, \\ 0 & \text{on } \partial\alpha \cap (\Gamma_D \setminus \Gamma_0) \,, \end{cases} \tag{4.10a}$$

$$(1+\theta)\nabla w \cdot \mathbf{n} + \sigma w = 0 \quad \text{on } \partial\alpha \cap \Gamma_D \,, \tag{4.10b}$$

$$\nabla w \cdot \mathbf{n} = 0 \quad \text{on } \partial\alpha \cap \Gamma_N \,. \tag{4.10c}$$

We note that when $\theta = -1$ the boundary conditions on $\partial\alpha \cap (\Gamma_D \cap \Gamma_0)$ become $w = -\psi(x,y)$ and $\sigma w = 0$ which are only compatible if either $\psi = 0$ on $\partial\alpha \cap (\Gamma_D \cap \Gamma_0)$ (which trivially gives $J_3(u) \equiv 0$) or if we choose $\sigma = 0$ on $\partial\alpha \cap (\Gamma_D \cap \Gamma_0)$.

However, we note that if we define

$$\hat{J}_3(u) = \int_{\Gamma_0} \theta\psi_3 \left(\theta \nabla u \cdot \mathbf{n} + \sigma u\right) \mathrm{d}s \,, \tag{4.11}$$

then

$$\hat{J}_3(u) = \int_{\Gamma_0} \psi_3 \left(\nabla u \cdot \mathbf{n} + \theta\sigma(u - g_\mathrm{D} + g_\mathrm{D})\right) \mathrm{d}s \tag{4.12}$$

$$= J_3(u) + \int_{\Gamma_0} \left(\psi_3 \theta \sigma g_\mathrm{D}\right) \mathrm{d}s \,, \tag{4.13}$$

using the facts that $u = g_\mathrm{D}$ on $\Gamma_0 \subset \Gamma_\mathrm{D}$ and that $\theta^2 = 1$. Since g_D is known, we may evaluate the second integral exactly (or approximate it using a quadrature rule which for our purposes we class as exact integration). Hence we may compute $J_3(u)$ by computing $\hat{J}_3(u)$ and subtracting the known quantity $\int_{\Gamma_0} \left(\psi_3 \theta \sigma g_\mathrm{D}\right) \mathrm{d}s$.

We may now define the weak formulation of the dual problem corresponding to the functional $\hat{J}_3(\cdot)$ to be

$$B(\phi, w) = \hat{J}_3(\phi) \,. \tag{4.14}$$

We find that the dual solution must satisfy

$$-\nabla^2 w = 0 \quad \text{in } \alpha \,, \tag{4.15}$$

with inter-element conditions given by (4.6) and boundary conditions given by

$$w = \begin{cases} -\psi_3(x,y) & \text{on } \partial\alpha \cap (\Gamma_D \cap \Gamma_0)\,, \\ 0 & \text{on } \partial\alpha \cap (\Gamma_D \setminus \Gamma_0)\,, \end{cases} \tag{4.16a}$$

$$(1+\theta)\nabla w \cdot \mathbf{n} + \sigma w = \begin{cases} \theta\sigma\psi_3(x,y) & \text{on } \partial\alpha \cap (\Gamma_D \cap \Gamma_0)\,, \\ 0 & \text{on } \partial\alpha \cap (\Gamma_D \setminus \Gamma_0)\,, \end{cases} \tag{4.16b}$$

$$\nabla w \cdot \mathbf{n} = 0 \quad \text{on } \partial\alpha \cap \Gamma_N\,. \tag{4.16c}$$

We emphasise that the SIPG method collapses to the formal dual problem while the NIPG method produces a problem whose solution differs from the formal dual solution on a set of zero measure. The regularity of the solution to the NIPG problem is lower than the solution to the formal dual problem.

5 Numerical Examples

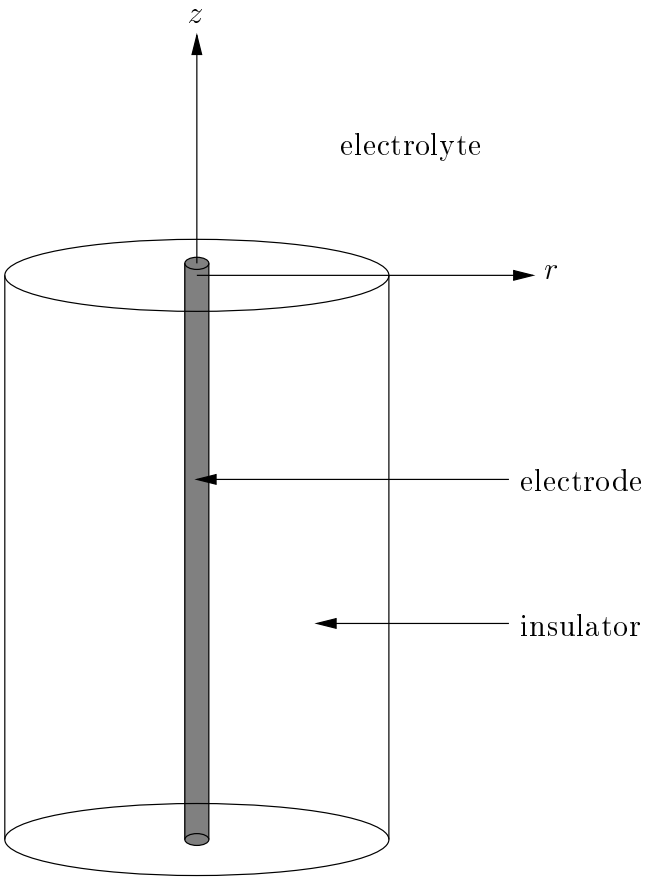

Figure 1: A microdisc electrode inlaid in an insulator.

We consider a problem which arises in electrochemistry. We consider an electrochemical cell in which the working electrode is a microdisc electrode which is inlaid

in an insulator as shown in Figure 1. The electrode radius is assumed to be small in comparison with the radius of the insulator which is thus assumed to be infinite. Here, we scale the radial independent variable r so that the electrode has radius $r = 1$. The top of the electrode is flush with the top of the insulator which we take to be the $z = 0$ plane. We then suppose that a constant potential is applied to the working electrode so that the oxidation reaction

$$A = B + e^- \tag{5.1}$$

takes place. This causes a current to flow and a particular quantity of interest is the steady state value of this current. This may be expressed as a linear functional of the steady state concentration values of species A. The normalised concentration values obey the steady state diffusion equation, which, due to axial symmetry, may be written in cylindrical polar coordinates as

$$-\nabla^2 u \;=\; \frac{\partial^2 u}{\partial r^2} + \frac{1}{r}\frac{\partial u}{\partial r} + \frac{\partial^2 u}{\partial z^2} \;=\; 0 \qquad \text{in } \Omega = (0,\infty)^2 \; . \tag{5.2}$$

The appropriate boundary conditions are

$$\begin{aligned} u &= 0, && r \le 1,\ z = 0, \\ \frac{\partial u}{\partial n} &= 0, && r > 1,\ z = 0, \\ & && r = 0,\ z \ge 0, \\ u &\sim 1 - 2/(\pi\sqrt{r^2+z^2}), && r, z \to \infty, \end{aligned} \tag{5.3}$$

where we have taken the electrode radius to be one by normalising the spatial coordinates. We note that the far field boundary conditions represent bulk concentration of species A there and the boundary condition on $z = 0$ for $r > 1$ represents the fact that no molecules of species A may leave through the insulator.

The form of the boundary conditions on $z = 0$ means that there is a boundary singularity at $(1, 0)$ (in other words $\partial u/\partial r$ is discontinuous there). This means that u has limited regularity (in fact $u \in H^{3/2-\epsilon}_{\rm loc}$, $0 < \epsilon < 1/2$) and so on a coarse uniform mesh standard finite element techniques will lead to a large error at this point which then degrades the accuracy of the current.

We shall calculate the normalised dimensionless current to the electrode which is given by

$$J_3(u) \;=\; \frac{\pi}{2}\int_0^1 \left(\frac{\partial u}{\partial z}\right)_{z=0} r\mathrm{d}r \; . \tag{5.4}$$

As described in the previous section we may instead compute

$$\hat{J}_3(u) \;=\; \int_{\Gamma_0} -\frac{\pi}{2}\theta\left(\theta\nabla u\cdot\mathbf{n} + \sigma u\right)\mathrm{d}s \; , \tag{5.5}$$

where Γ_0 represents the electrode surface, i.e.

$$\Gamma_0 \;=\; \{(r,z) \in \Gamma_{\rm D} :\ 0 \le r \le 1,\ z = 0\} \; . \tag{5.6}$$

The exact solution to the steady state problem described by (5.2) and (5.3) was given by Saito [16] as

$$u = 1 - \frac{2}{\pi}\int_0^\infty \frac{\sin m}{m} J_0(rm)e^{-zm}\mathrm{d}m \ , \tag{5.7}$$

where J_0 is the zeroth order Bessel function. Hence the non-dimensional current is given by $J_3(u) = 1$.

Crank and Furzeland [5] rewrote Saito's solution in the more convenient form

$$u \ = \ 1 - \frac{2}{\pi}\sin^{-1}\left\{\frac{2}{\sqrt{z^2+(1+r)^2}+\sqrt{z^2+(1-r)^2}}\right\} \ . \tag{5.8}$$

To illustrate our numerical method we shall solve the problem in the region $\Omega_s = [0, r_{\max}]\times[0, z_{\max}]$. We shall then use the exact solution as given by Crank and Furzeland as the boundary condition on $r = r_{\max}$ and $z = z_{\max}$. We shall choose $r_{\max} = z_{\max} = 2$.

To illustrate the method and convergence rates we shall also compute two further functionals, the integral over the domain of the solution and a point value in the interior of the domain

$$J_1(u) \ = \ \int_{\Omega_s} u\mathrm{d}\Omega \ , \tag{5.9}$$

$$J_2(u) \ = \ u(1/3, 1/3) \ . \tag{5.10}$$

The exact values of the functionals can be found to be $J_1(u) = 2.426131$ and $J_2(u) = 0.214987$.

5.1 The Dual Solutions

In Figure 2 we show the dual solutions computed using DGFEM with a fixed polynomial degree of 2 in each element and with 8 mesh spacings in each coordinate direction. The formal dual solution is well approximated by the dual based on $\hat{J}_3(\cdot)$ and the SIPG scheme in the sense that the numerical solution looks very similar to a continuous finite element solution to the formal dual problem. The numerical solution corresponding to the problem based on the SIPG scheme and the functional $\hat{J}_3(\cdot)$ is shown in Figure 2(a). In Figure 2(b) we show the numerical solution to the dual problem based on SIPG and the functional $J_3(\cdot)$. We see that this differs considerably from the formal dual solution, especially near the electrode surface where the boundary conditions are inconsistent. The behaviour of this solution is dependent upon the choice of the constant C_σ in the definition of σ (2.8). Here we have chosen $C_\sigma = 10$. Decreasing this increases the peak value of the dual solution and decreases the value on the electrode surface. Increasing the value of C_σ reduces the peak height and increases the value of the solution on the electrode surface. In the limit as $C_\sigma \to \infty$ the peak height of the dual solution is $\pi/2$ (the value of the formal dual solution on the electrode surface) and the value of the dual solution on the electrode surface is zero. In Figures 2(c) and 2(d) we show the numerical

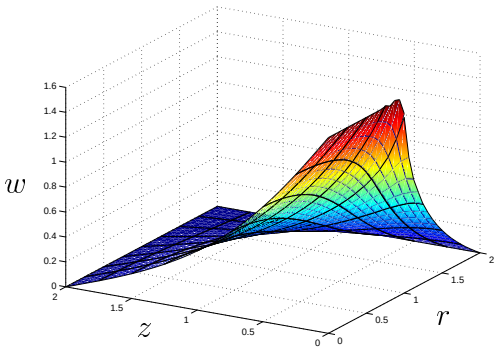

(a) Dual based on $\hat{J}_3(\cdot)$ and SIPG.

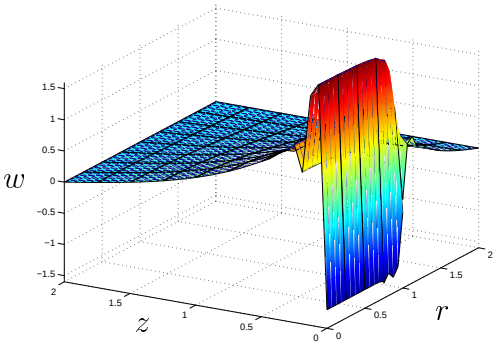

(b) Dual based on $J_3(\cdot)$ and SIPG.

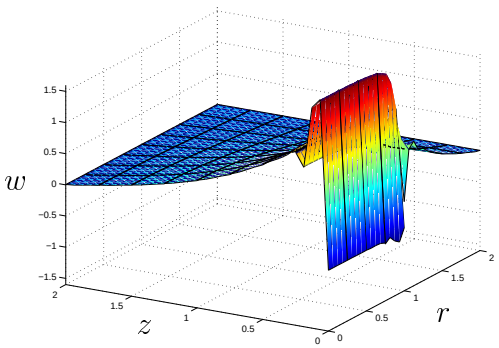

(c) Dual based on $\hat{J}_3(\cdot)$ and NIPG.

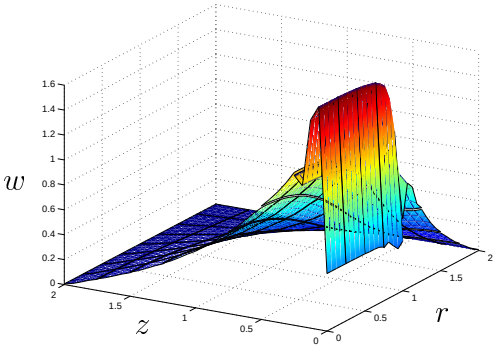

(d) Dual based on $J_3(\cdot)$ and NIPG.

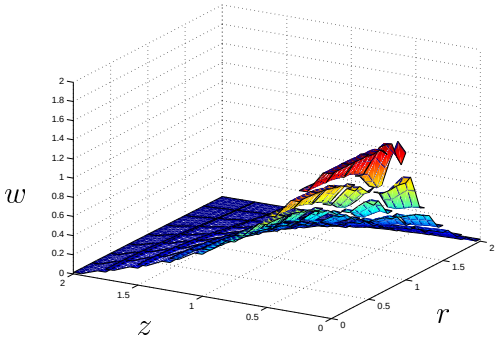

(e) Dual based on $\hat{J}_3(\cdot)$ and NIPG with $\sigma = 0$.

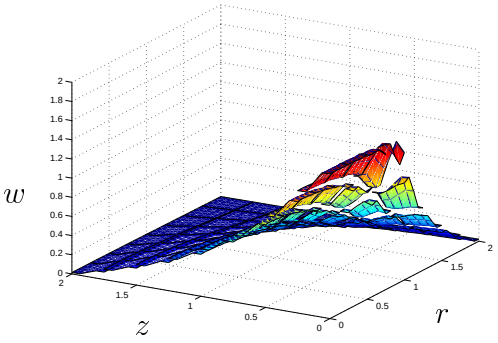

(f) Dual based on $J_3(\cdot)$ and NIPG with $\sigma = 0$.

Figure 2: The dual solutions on an 8×8 mesh with $p = 2$ for the functionals $J_3(\cdot)$ and $\hat{J}_3(\cdot)$.

solutions to the dual problem based on NIPG and $\hat{J}_3(\cdot)$ and $J_3(\cdot)$, respectively with $C_\sigma = 10$. Figures 2(e) and 2(f) show the corresponding solutions with $C_\sigma = 0$. These show more clearly the effect of the inter-element condition (4.6a) which requires the average gradient of the solution to be zero across interior edges. We also note that in the case when σ is non-zero the boundary conditions on the electrode surface are

$$w = -\psi_3(x,y) \tag{5.11}$$

$$2\nabla w \cdot \mathbf{n} + \sigma w = \delta\sigma\psi_3(x,y) \tag{5.12}$$

where $\delta = 0$ if we are considering the problem relating to $J_3(\cdot)$ and $\delta = 1$ if we are considering the problem relating to $\hat{J}_3(\cdot)$. Substituting (5.11) into (5.12) gives

$$\nabla w \cdot \mathbf{n} = \frac{\sigma}{2}\psi_3(x,y)(\delta+1)\,, \tag{5.13}$$

and since $\psi_3 = -\pi/2$ on the electrode surface this tells us that the dual solution should increase away from the electrode surface which is indeed the case in Figures 2(c) and 2(d).

In Figure 3 we show the convergence rates of the linear functionals using SIPG and NIPG. As expected we achieve $\mathcal{O}(h)$ convergence for each of the functionals $J_1(u_{\text{SIPG}})$, $J_2(u_{\text{SIPG}})$, $\hat{J}_3(u_{\text{SIPG}})$ and the original form of the third functional $J_3(u_{\text{SIPG}})$ only achieves $\mathcal{O}(h^{1/2})$ convergence. Using NIPG we see that $J_3(u_{\text{NIPG}})$ and $\hat{J}_3(u_{\text{NIPG}})$ achieve $\mathcal{O}(h^{1/2})$ convergence as predicted by the theory. However, $J_1(u_{\text{NIPG}})$ and $J_2(u_{\text{NIPG}})$ do better than theory predicts achieving $\mathcal{O}(h)$ convergence. In the case of $J_1(u_{\text{NIPG}})$ this is not surprising since

$$|J_1(u-u_{\text{NIPG}})| = \left|\int_{\Omega_s}\psi_1(u-u_{\text{NIPG}})\mathrm{d}\Omega\right| \tag{5.14}$$

$$\leq \|\psi_1\|_{L_2(\Omega_s)}\|u-u_{\text{NIPG}}\|_{L_2(\Omega_s)} \tag{5.15}$$

$$= C\|u-u_{\text{NIPG}}\|_{L_2(\Omega_s)} \tag{5.16}$$

where $C = \|\psi_1\|_{L_2(\Omega_s)}$ is a positive constant and $\psi_1(r,z) \equiv 1$. Thus we expect the rate of convergence of the functional to be no smaller than the rate of convergence of the error in the L_2 norm which has previously been observed to be $\mathcal{O}(h^a)$ where

$$a = \begin{cases} \min(p+1, s-1/2) & p \text{ odd} \\ \min(p, s-1/2) & p \text{ even} \end{cases} \tag{5.17}$$

where $u \in H^s(\Omega)$ [13].

6 Conclusions

In this work we have described how to approximate a linear functional of the solution of an elliptic partial differential equation using a discontinuous Galerkin finite element method. We used a symmetric interior penalty Galerkin method (SIPG) which ensured

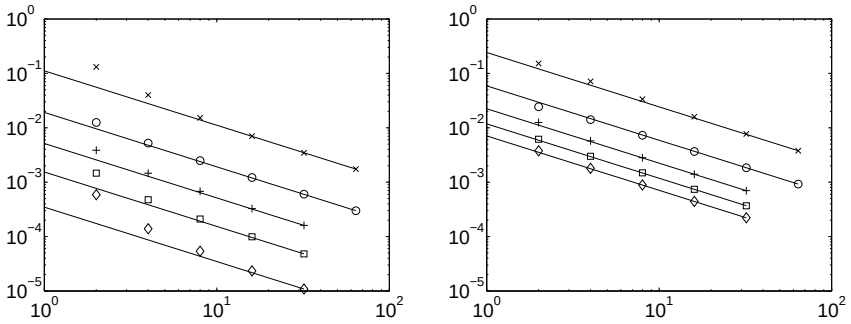

(a) Convergence of $J_1(u_{\mathrm{SIPG}})$.

(b) Convergence of $J_1(u_{\mathrm{NIPG}})$.

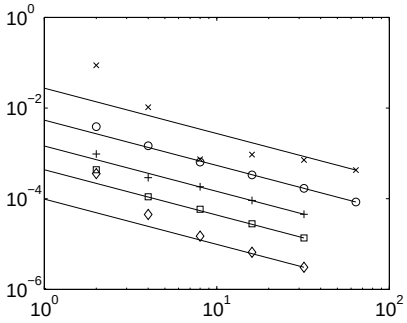

(c) Convergence of $J_2(u_{\mathrm{SIPG}})$.

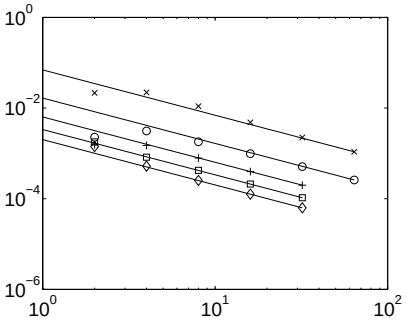

(d) Convergence of $J_2(u_{\mathrm{NIPG}})$.

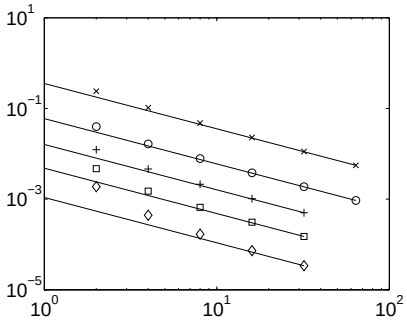

(e) Convergence of $\hat{J}_3(u_{\mathrm{SIPG}})$.

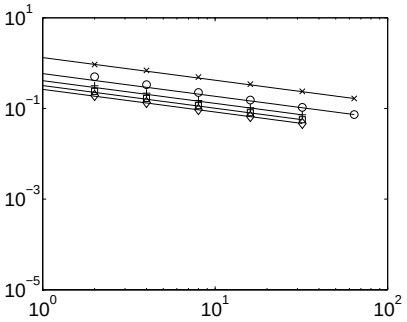

(f) Convergence of $\hat{J}_3(u_{\mathrm{NIPG}})$.

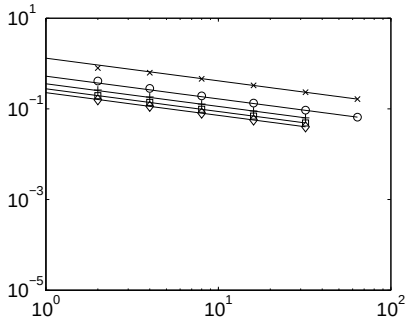

(g) Convergence of $J_3(u_{\mathrm{SIPG}})$.

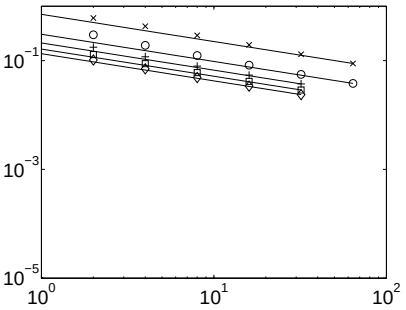

(h) Convergence of $J_3(u_{\mathrm{NIPG}})$.

Figure 3: Convergence of the errors in the functionals using SIPG and NIPG using polynomial degrees $p = 1$ ($\times$); $p = 2$ ($\circ$); $p = 3$ ($+$); $p = 4$ ($\square$); $p = 5$ ($\diamond$).

that adjoint consistency was achieved; it was shown that this was vital if we were to obtain the optimal rate of convergence of the numerical approximation of the functional to the exact solution. We also showed how, if the functional depended on the derivative of the solution, rather than the solution itself, we could re-write the functional in a formulation which was equivalent at the continuous level, but again ensured that adjoint consistency was achieved and we thus obtained optimal rates of convergence.

7 Acknowledgements

The authors are pleased to acknowledge the financial support of the EPSRC (Grant Number: GR/R17041).

References

[1] I. Babuška and A. Miller, 1984. The post-processing approach in the finite element method — Part 1: Calculation of displacements, stresses and other higher derivatives of the displacements. *Int. J. Num. Meth. Engnrg.*, **20**(6): 1085.

[2] I. Babuška and A. Miller, 1984. The post-processing approach in the finite element method — Part 2: The calculation of stress intensity factors. *Int. J. Num. Meth. Engnrg.*, **20**(6): 1111.

[3] I. Babuška and A. Miller, 1984. The post-processing approach in the finite element method — Part 3: A posteriori error estimates and adaptive mesh selection. *Int. J. Num. Meth. Engnrg.*, **20**(12): 2311.

[4] B. Cockburn, G.E. Karniadakis and C.-W. Shu, 2000. The development of discontinuous Galerkin methods. *In* B. Cockburn, G.E. Karniadakis and C.-W. Shu, editors, *Lecture Notes in Computational Science and Engineering*, Volume 11. Springer.

[5] J. Crank and R.M. Furzeland, 1977. The Treatment of Boundary Singularities in Axially Symmetric Problems Containing Discs. *J. Inst. Maths. Applics*, **20**(3): 355.

[6] C. Fuhrer and R. Rannacher, 1996. Error analysis for the finite element approximation of a radiative transfer model. *RAIRO Mathematical Modelling and Numerical Analysis*, **30**(6): 743.

[7] M. Giles, M.G. Larson, J.M. Levenstam and E. Süli, 1997. Adaptive error control for finite element approximations of the lift and drag coefficients in viscous flow. Technical Report NA97/06, Oxford University Computing Laboratory, Wolfson Building, Parks Road, Oxford OX1 3QD.

[8] K. Harriman, D.J. Gavaghan, P. Houston and E. Süli, 2000. Adaptive Finite Element Simulation of Currents at Microelectrodes to a Guaranteed Accuracy. Application to a Simple Model Problem. *Electrochem. Commun.*, **2**(3): 150.

[9] K. Harriman, D.J. Gavaghan, P. Houston and E. Süli, 2000. Adaptive Finite Element Simulation of Currents at Microelectrodes to a Guaranteed Accuracy. Theory. *Electrochem. Commun.*, **2**(3): 157.

[10] K. Harriman, P. Houston, W. Senior and E. Süli, 2003. *hp*-Version Discontiuous Galerkin Finite Element Methods with Interior Penalty for Partial Differential Equations with Nonnegative Characteristic Form. *In* C.-W. Shu, T. Tang and S.-Y. Cheng, editors, *Recent Advances in Scientific Computing and Partial Differential Equations*, Volume 330 of *Contemporary Mathematics*, page 89. AMS, Providence, RI.

[11] P. Houston, Ch. Schwab and E. Süli, 2002. Discontinuous *hp*-finite element methods for advection–diffusion–reaction problems. *SIAM J. Numer. Anal.*, **39**(6): 2133.

[12] J. Nitsche, 1971. Über ein Variationsprinzip zur Lösung von Dirichlet-Problemen bei Verwendung von Teilräumen, die keinen Randbedingungen unterworfen sind. *Abh. Math. Sem. Univ. Hamburg*, **36**: 9.

[13] J. Tinsley Oden, Ivo Babuška and Carlos Erik Baumann, 1998. A discontinuous *hp* finite element method for diffusion problems. *J. Comput. Phys.*, **146**: 491–519.

[14] S. Prudhomme, F. Pascal, J.T. Oden and A. Romkes, 2000. Review of *A Priori* Error Estimation for Discontinuous Galerkin Methods. Technical Report 00-27, Texas Institute for Computational and Applied Mathematics, University of Texas at Austin.

[15] W.H. Reed and T.R. Hill, 1973. Triangular Mesh Methods for the Neutron Transport Equation. Technical Report LA-UR-73-479, Los Alamos Scientific Laboratory, Los Alamos, NM.

[16] Y. Saito, 1968. A Theoretical Study on the Diffusion Current at the Stationary Electrodes of Circular and Narrow Band Types. *Rev. Polarogr. (Jpn)*, **15**(6): 177.